EUROPEAN ORGANIZATION FOR NUCLEAR RESEARCH

CERN–PPE/97–62

3 June 1997

Observation of Charge-Ordering in Particle Production in Hadronic Z^0 Decay

DELPHI Collaboration

Abstract

Analysis of the rapidity structure of charge correlations in hadronic events from Z^0 decays gives evidence for chain-like charge-ordering of particle production along the thrust axis, as predicted by 'QCD-motivated' string-like fragmentation models.

(To be submitted to Phys. Lett. B)

P.Abreu[21], W.Adam[49], T.Adye[36], P.Adzic[11], G.D.Alekseev[16], R.Alemany[48], P.P.Allport[22], S.Almehed[24], U.Amaldi[9], S.Amato[46], P.Andersson[43], A.Andreazza[9], P.Antilogus[9], W-D.Apel[17], Y.Arnoud[14], B.Åsman[43], J-E.Augustin[25], A.Augustinus[30], P.Baillon[9], P.Bambade[19], F.Barao[21], M.Barbi[46], G.Barbiellini[45], D.Y.Bardin[16], G.Barker[9], A.Baroncelli[39], O.Barring[24], M.J.Bates[36], M.Battaglia[15], M.Baubillier[23], J.Baudot[38], K-H.Becks[51], M.Begalli[6], P.Beilliere[8], Yu.Belokopytov[9,52], A.C.Benvenuti[5], C.Berat[14], M.Berggren[46], D.Bertini[25], D.Bertrand[2], M.Besancon[38], F.Bianchi[44], M.Bigi[44], M.S.Bilenky[16], P.Billoir[23], M-A.Bizouard[19], D.Bloch[10], M.Blume[51], M.Bonesini[27], W.Bonivento[27], P.S.L.Booth[22], A.W.Borgland[4], G.Borisov[38,41], C.Bosio[39], O.Botner[47], E.Boudinov[30], B.Bouquet[19], C.Bourdarios[19], T.J.V.Bowcock[22], M.Bozzo[13], P.Branchini[39], K.D.Brand[35], T.Brenke[51], R.A.Brenner[47], C.Bricman[2], R.C.A.Brown[9], P.Bruckman[18], J-M.Brunet[8], L.Bugge[32], T.Buran[32], T.Burgsmueller[51], P.Buschmann[51], S.Cabrera[48], M.Caccia[27], M.Calvi[27], A.J.Camacho Rozas[40], T.Camporesi[9], V.Canale[37], M.Canepa[13], F.Cao[2], F.Carena[9], L.Carroll[22], C.Caso[13], M.V.Castillo Gimenez[48], A.Cattai[9], F.R.Cavallo[5], V.Chabaud[9], Ph.Charpentier[9], L.Chaussard[25], P.Checchia[35], G.A.Chelkov[16], M.Chen[2], R.Chierici[44], P.Chliapnikov[41], P.Chochula[7], V.Chorowicz[25], J.Chudoba[29], V.Cindro[42], P.Collins[9], R.Contri[13], E.Cortina[48], G.Cosme[19], F.Cossutti[45], J-H.Cowell[22], H.B.Crawley[1], D.Crennell[36], G.Crosetti[13], J.Cuevas Maestro[33], S.Czellar[15], J.Dahm[51], B.Dalmagne[19], G.Damgaard[28], P.D.Dauncey[36], M.Davenport[9], W.Da Silva[23], A.Deghorain[2], G.Della Ricca[45], P.Delpierre[26], N.Demaria[34], A.De Angelis[9], W.De Boer[17], S.De Brabandere[2], C.De Clercq[2], C.De La Vaissiere[23], B.De Lotto[45], A.De Min[35], L.De Paula[46], H.Dijkstra[9], L.Di Ciaccio[37], A.Di Diodato[37], A.Djannati[8], J.Dolbeau[8], K.Doroba[50], M.Dracos[10], J.Drees[51], K.-A.Drees[51], M.Dris[31], J-D.Durand[25,9], D.Edsall[1], R.Ehret[17], G.Eigen[4], T.Ekelof[47], G.Ekspong[43], M.Elsing[9], J-P.Engel[10], B.Erzen[42], M.Espirito Santo[21], E.Falk[24], G.Fanourakis[11], D.Fassouliotis[45], M.Feindt[9], A.Fenyuk[41], P.Ferrari[27], A.Ferrer[48], S.Fichet[23], T.A.Filippas[31], A.Firestone[1], P.-A.Fischer[10], H.Foeth[9], E.Fokitis[31], F.Fontanelli[13], F.Formenti[9], B.Franek[36], A.G.Frodesen[4], R.Fruhwirth[49], F.Fulda-Quenzer[19], J.Fuster[48], A.Galloni[22], D.Gamba[44], M.Gandelman[46], C.Garcia[48], J.Garcia[40], C.Gaspar[9], U.Gasparini[35], Ph.Gavillet[9], E.N.Gazis[31], D.Gele[10], J-P.Gerber[10], L.Geryukov[41], R.Gokieli[50], B.Golob[42], P.Goncalves[21], G.Gopal[36], L.Gorn[1], M.Gorski[50], Yu.Gouz[44,52], V.Gracco[13], E.Graziani[39], C.Green[22], A.Grefrath[51], P.Gris[38], G.Grosdidier[19], K.Grzelak[50], M.Gunther[47], J.Guy[36], F.Hahn[9], S.Hahn[51], Z.Hajduk[18], A.Hallgren[47], K.Hamacher[51], F.J.Harris[34], V.Hedberg[24], R.Henriques[21], J.J.Hernandez[48], P.Herquet[2], H.Herr[9], T.L.Hessing[34], J.-M.Heuser[51], E.Higon[48], S-O.Holmgren[43], P.J.Holt[34], D.Holthuizen[30], S.Hoorelbeke[2], M.Houlden[22], J.Hrubec[49], K.Huet[2], K.Hultqvist[43], J.N.Jackson[22], R.Jacobsson[43], P.Jalocha[9], R.Janik[7], Ch.Jarlskog[24], G.Jarlskog[24], P.Jarry[38], B.Jean-Marie[19], E.K.Johansson[43], L.Jonsson[24], P.Jonsson[24], C.Joram[9], P.Juillot[10], M.Kaiser[17], F.Kapusta[23], K.Karafasoulis[11], S.Katsanevas[25], E.C.Katsoufis[31], R.Keranen[4], Yu.Khokhlov[41], B.A.Khomenko[16], N.N.Khovanski[16], B.King[22], N.J.Kjaer[30], O.Klapp[51], H.Klein[9], P.Kluit[30], D.Knoblauch[17], P.Kokkinias[11], A.Konopliannikov[41], M.Koratzinos[9], K.Korcyl[18], V.Kostioukhine[41], C.Kourkoumelis[3], O.Kouznetsov[13,16], M.Krammer[49], C.Kreuter[9], I.Kronkvist[24], Z.Krumstein[16], W.Krupinski[18], P.Kubinec[7], W.Kucewicz[18], K.Kurvinen[15], C.Lacasta[9], I.Laktineh[25], J.W.Lamsa[1], L.Lanceri[45], D.W.Lane[1], P.Langefeld[51], J-P.Laugier[38], R.Lauhakangas[15], F.Ledroit[14], V.Lefebure[2], C.K.Legan[1], A.Leisos[11], R.Leitner[29], J.Lemonne[2], G.Lenzen[51], V.Lepeltier[19], T.Lesiak[18], J.Libby[34], D.Liko[9], A.Lipniacka[43], I.Lippi[35], B.Loerstad[24], J.G.Loken[34], J.M.Lopez[40], D.Loukas[11], P.Lutz[38], L.Lyons[34], J.MacNaughton[49], G.Maehlum[17], J.R.Mahon[6], A.Maio[21], T.G.M.Malmgren[43], V.Malychev[16], F.Mandl[49], J.Marco[40], R.Marco[40], B.Marechal[46], M.Margoni[35], J-C.Marin[9], C.Mariotti[9], A.Markou[11], C.Martinez-Rivero[33], F.Martinez-Vidal[48], S.Marti i Garcia[22], J.Masik[29], F.Matorras[40], C.Matteuzzi[27], G.Matthiae[37], M.Mazzucato[35], M.Mc Cubbin[22], R.Mc Kay[1], R.Mc Nulty[9], G.Mc Pherson[22], J.Medbo[47], C.Meroni[27], S.Meyer[17], W.T.Meyer[1], A.Miagkov[41], M.Michelotto[35], E.Migliore[44], L.Mirabito[25], W.A.Mitaroff[49], U.Mjoernmark[24], T.Moa[43], R.Moeller[28], K.Moenig[9], M.R.Monge[13], P.Morettini[13], H.Mueller[17], K.Muenich[51], M.Mulders[30], L.M.Mundim[6], W.J.Murray[36], B.Muryn[14,18], G.Myatt[34], T.Myklebust[32], F.Naraghi[14], F.L.Navarria[5], S.Navas[48], K.Nawrocki[50], P.Negri[27], S.Nemecek[12], W.Neumann[51], N.Neumeister[49], R.Nicolaidou[3], B.S.Nielsen[28], M.Nieuwenhuizen[30], V.Nikolaenko[10], M.Nikolenko[10,16], P.Niss[43], A.Nomerotski[35], A.Normand[22], A.Nygren[24], W.Oberschulte-Beckmann[17], V.Obraztsov[41], A.G.Olshevski[16], A.Onofre[21], R.Orava[15], G.Orazi[10], K.Osterberg[15], A.Ouraou[38], P.Paganini[19], M.Paganoni[9,27], R.Pain[23], H.Palka[18], Th.D.Papadopoulou[31], K.Papageorgiou[11], L.Pape[9], C.Parkes[34], F.Parodi[13], U.Parzefall[22], A.Passeri[39], M.Pegoraro[35], L.Peralta[21], H.Pernegger[49], M.Pernicka[49], A.Perrotta[5], C.Petridou[45], A.Petrolini[13], H.T.Phillips[36], G.Piana[13], F.Pierre[38], M.Pimenta[21], T.Podobnik[34], O.Podobrin[9], M.E.Pol[6], G.Polok[18], P.Poropat[45], V.Pozdniakov[16], P.Privitera[37], N.Pukhaeva[16], A.Pullia[27], D.Radojicic[34], S.Ragazzi[27], H.Rahmani[31], P.N.Ratoff[20], A.L.Read[32], M.Reale[51], P.Rebecchi[9], N.G.Redaelli[27], M.Regler[49], D.Reid[9], R.Reinhardt[51], P.B.Renton[34], L.K.Resvanis[3], F.Richard[19], J.Ridky[12], G.Rinaudo[44], O.Rohne[32], A.Romero[44], P.Ronchese[35], L.Roos[23], E.I.Rosenberg[1], P.Rosinsky[7], P.Roudeau[19], T.Rovelli[5], V.Ruhlmann-Kleider[38], A.Ruiz[40], K.Rybicki[18], H.Saarikko[15], Y.Sacquin[38], A.Sadovsky[16], G.Sajot[14], J.Salt[48], M.Sannino[13], H.Schneider[17], U.Schwickerath[17], M.A.E.Schyns[51], G.Sciolla[44], F.Scuri[45], P.Seager[20], Y.Sedykh[16], A.M.Segar[34], A.Seitz[17], R.Sekulin[36], L.Serbelloni[37], R.C.Shellard[6], A.Sheridan[22], P.Siegrist[9,38], R.Silvestre[38], F.Simonetto[35], A.N.Sisakian[16], T.B.Skaali[32], G.Smadja[25], N.Smirnov[41], O.Smirnova[24], G.R.Smith[36], A.Sokolov[41], O.Solovianov[41], R.Sosnowski[50], D.Souza-Santos[6], T.Spassov[21], E.Spiriti[39], P.Sponholz[51], S.Squarcia[13], D.Stampfer[9], C.Stanescu[39], S.Stanic[42], S.Stapnes[32], I.Stavitski[35], K.Stevenson[34], A.Stocchi[19], J.Strauss[49], R.Strub[10], B.Stugu[4], M.Szczekowski[50], M.Szeptycka[50], T.Tabarelli[27], J.P.Tavernet[23], E.Tcherniaev[41], F.Tegenfeldt[47], F.Terranova[27], J.Thomas[34], A.Tilquin[26], J.Timmermans[30], L.G.Tkatchev[16], T.Todorov[10], S.Todorova[10], D.Z.Toet[30], A.Tomaradze[2], B.Tome[21], A.Tonazzo[27], L.Tortora[39], G.Transtromer[24], D.Treille[9], G.Tristram[8], A.Trombini[19], C.Troncon[27], A.Tsirou[9], M-L.Turluer[38], I.A.Tyapkin[16], M.Tyndel[36], S.Tzamarias[11], B.Ueberschaer[51], O.Ullaland[9], V.Uvarov[41], G.Valenti[5], E.Vallazza[45], G.W.Van Apeldoorn[30], P.Van Dam[30], J.Van Eldik[30], A.Van Lysebetten[2], N.Vassilopoulos[34], G.Vegni[27], L.Ventura[35], W.Venus[36], F.Verbeure[2], M.Verlato[35], L.S.Vertogradov[16], D.Vilanova[38], P.Vincent[25], L.Vitale[45], A.S.Vodopyanov[16], V.Vrba[12], H.Wahlen[51], C.Walck[43], C.Weiser[17], A.M.Wetherell[9], D.Wicke[51], J.H.Wickens[2], M.Wielers[17], G.R.Wilkinson[9], W.S.C.Williams[34], M.Winter[10], M.Witek[18], T.Wlodek[19], J.Yi[1], K.Yip[34], O.Yushchenko[41], F.Zach[25], A.Zaitsev[41], A.Zalewska[9], P.Zalewski[50], D.Zavrtanik[42], E.Zevgolatakos[11], N.I.Zimin[16], G.C.Zucchelli[43], G.Zumerle[35]

[1]Department of Physics and Astronomy, Iowa State University, Ames IA 50011-3160, USA
[2]Physics Department, Univ. Instelling Antwerpen, Universiteitsplein 1, B-2610 Wilrijk, Belgium
and IIHE, ULB-VUB, Pleinlaan 2, B-1050 Brussels, Belgium
and Faculté des Sciences, Univ. de l'Etat Mons, Av. Maistriau 19, B-7000 Mons, Belgium
[3]Physics Laboratory, University of Athens, Solonos Str. 104, GR-10680 Athens, Greece
[4]Department of Physics, University of Bergen, Allégaten 55, N-5007 Bergen, Norway
[5]Dipartimento di Fisica, Università di Bologna and INFN, Via Irnerio 46, I-40126 Bologna, Italy
[6]Centro Brasileiro de Pesquisas Físicas, rua Xavier Sigaud 150, RJ-22290 Rio de Janeiro, Brazil
and Depto. de Física, Pont. Univ. Católica, C.P. 38071 RJ-22453 Rio de Janeiro, Brazil
and Inst. de Física, Univ. Estadual do Rio de Janeiro, rua São Francisco Xavier 524, Rio de Janeiro, Brazil
[7]Comenius University, Faculty of Mathematics and Physics, Mlynska Dolina, SK-84215 Bratislava, Slovakia
[8]Collège de France, Lab. de Physique Corpusculaire, IN2P3-CNRS, F-75231 Paris Cedex 05, France
[9]CERN, CH-1211 Geneva 23, Switzerland
[10]Institut de Recherches Subatomiques, IN2P3 - CNRS/ULP - BP20, F-67037 Strasbourg Cedex, France
[11]Institute of Nuclear Physics, N.C.S.R. Demokritos, P.O. Box 60228, GR-15310 Athens, Greece
[12]FZU, Inst. of Physics of the C.A.S. High Energy Physics Division, Na Slovance 2, 180 40, Praha 8, Czech Republic
[13]Dipartimento di Fisica, Università di Genova and INFN, Via Dodecaneso 33, I-16146 Genova, Italy
[14]Institut des Sciences Nucléaires, IN2P3-CNRS, Université de Grenoble 1, F-38026 Grenoble Cedex, France
[15]Helsinki Institute of Physics, HIP, P.O. Box 9, FIN-00014 Helsinki, Finland
[16]Joint Institute for Nuclear Research, Dubna, Head Post Office, P.O. Box 79, 101 000 Moscow, Russian Federation
[17]Institut für Experimentelle Kernphysik, Universität Karlsruhe, Postfach 6980, D-76128 Karlsruhe, Germany
[18]Institute of Nuclear Physics and University of Mining and Metalurgy, Ul. Kawiory 26a, PL-30055 Krakow, Poland
[19]Université de Paris-Sud, Lab. de l'Accélérateur Linéaire, IN2P3-CNRS, Bât. 200, F-91405 Orsay Cedex, France
[20]School of Physics and Chemistry, University of Lancaster, Lancaster LA1 4YB, UK
[21]LIP, IST, FCUL - Av. Elias Garcia, 14-1^o, P-1000 Lisboa Codex, Portugal
[22]Department of Physics, University of Liverpool, P.O. Box 147, Liverpool L69 3BX, UK
[23]LPNHE, IN2P3-CNRS, Universités Paris VI et VII, Tour 33 (RdC), 4 place Jussieu, F-75252 Paris Cedex 05, France
[24]Department of Physics, University of Lund, Sölvegatan 14, S-22363 Lund, Sweden
[25]Université Claude Bernard de Lyon, IPNL, IN2P3-CNRS, F-69622 Villeurbanne Cedex, France
[26]Univ. d'Aix - Marseille II - CPP, IN2P3-CNRS, F-13288 Marseille Cedex 09, France
[27]Dipartimento di Fisica, Università di Milano and INFN, Via Celoria 16, I-20133 Milan, Italy
[28]Niels Bohr Institute, Blegdamsvej 17, DK-2100 Copenhagen 0, Denmark
[29]NC, Nuclear Centre of MFF, Charles University, Areal MFF, V Holesovickach 2, 180 00, Praha 8, Czech Republic
[30]NIKHEF, Postbus 41882, NL-1009 DB Amsterdam, The Netherlands
[31]National Technical University, Physics Department, Zografou Campus, GR-15773 Athens, Greece
[32]Physics Department, University of Oslo, Blindern, N-1000 Oslo 3, Norway
[33]Dpto. Fisica, Univ. Oviedo, Avda. Calvo Sotelo, S/N-33007 Oviedo, Spain, (CICYT-AEN96-1681)
[34]Department of Physics, University of Oxford, Keble Road, Oxford OX1 3RH, UK
[35]Dipartimento di Fisica, Università di Padova and INFN, Via Marzolo 8, I-35131 Padua, Italy
[36]Rutherford Appleton Laboratory, Chilton, Didcot OX11 OQX, UK
[37]Dipartimento di Fisica, Università di Roma II and INFN, Tor Vergata, I-00173 Rome, Italy
[38]CEA, DAPNIA/Service de Physique des Particules, CE-Saclay, F-91191 Gif-sur-Yvette Cedex, France
[39]Istituto Superiore di Sanità, Ist. Naz. di Fisica Nucl. (INFN), Viale Regina Elena 299, I-00161 Rome, Italy
[40]Instituto de Fisica de Cantabria (CSIC-UC), Avda. los Castros, S/N-39006 Santander, Spain, (CICYT-AEN96-1681)
[41]Inst. for High Energy Physics, Serpukov P.O. Box 35, Protvino, (Moscow Region), Russian Federation
[42]J. Stefan Institute, Jamova 39, SI-1000 Ljubljana, Slovenia and Department of Astroparticle Physics, School of Environmental Sciences, Kostanjeviska 16a, Nova Gorica, SI-5000 Slovenia,
and Department of Physics, University of Ljubljana, SI-1000 Ljubljana, Slovenia
[43]Fysikum, Stockholm University, Box 6730, S-113 85 Stockholm, Sweden
[44]Dipartimento di Fisica Sperimentale, Università di Torino and INFN, Via P. Giuria 1, I-10125 Turin, Italy
[45]Dipartimento di Fisica, Università di Trieste and INFN, Via A. Valerio 2, I-34127 Trieste, Italy
and Istituto di Fisica, Università di Udine, I-33100 Udine, Italy
[46]Univ. Federal do Rio de Janeiro, C.P. 68528 Cidade Univ., Ilha do Fundão BR-21945-970 Rio de Janeiro, Brazil
[47]Department of Radiation Sciences, University of Uppsala, P.O. Box 535, S-751 21 Uppsala, Sweden
[48]IFIC, Valencia-CSIC, and D.F.A.M.N., U. de Valencia, Avda. Dr. Moliner 50, E-46100 Burjassot (Valencia), Spain
[49]Institut für Hochenergiephysik, Österr. Akad. d. Wissensch., Nikolsdorfergasse 18, A-1050 Vienna, Austria
[50]Inst. Nuclear Studies and University of Warsaw, Ul. Hoza 69, PL-00681 Warsaw, Poland
[51]Fachbereich Physik, University of Wuppertal, Postfach 100 127, D-42097 Wuppertal, Germany
[52]On leave of absence from IHEP Serpukhov

1 Introduction

The phenomenon of chain-like flavor-ordered particle production is a general prediction of 'QCD-motivated' string-fragmentation models for jet hadronisation [1]. Hadronic events produced from e^+e^- annihilation yield two primary quarks ($q\bar{q}$) which carry opposite quantum numbers and which are at the end points of a chain. The chain (or string) is formed from the color neutral system which stretches (due to linear confinement) between the primary quarks. Hadronisation results from the break-up of the string as the two primary quarks move apart. The breaks occur between a quark and antiquark forming a virtual flavor-neutral $q\bar{q}$ pair produced from potential energy in the string. Hadrons produced by the model are in strict flavor ordering, called 'rank' [2], as illustrated in Fig. 1a where, on the left side, the $u\bar{d}$ becomes the first rank particle π^+, the $d\bar{u}$ the second rank particle π^-, etc. (see also Fig. 1b for a description of rank). Flavor ordering is a result of the fact that two adjacent-ranked hadrons share a $q\bar{q}$ pair. Owing to the chain-like ordering, charged hadrons (regardless of flavor) are predicted to be produced with an *alternating charge structure* along the entire chain.

It should be noted that although ordering in rank is strict, the corresponding ordering in rapidity is not. This is because of the softness of the fragmentation function, hard gluon production, p_T effects, and cluster/resonance decays, all of which can mix the order in rapidity of the detected hadrons. Nevertheless, a weak coupling between rank and relative position in rapidity is predicted and can be studied experimentally.

Previous studies at lower energy [3] have shown evidence for charge rank ordering at the ends of the rapidity chain. This paper gives evidence for the existence of charge-ordered hadron production in the rapidity variable measured along the thrust axis in hadronic Z^0 decays in e^+e^- events at LEP.

In addition, the data are compared to predictions of the JETSET 7.3 [4] and HERWIG 5.5 [5] models. From the above discussion, it is clear that the string-model JETSET is expected to yield charge-ordering. But HERWIG, although a cluster model, also has 'string-like' features. The concept of 'preconfinement' is used to produce clusters, which are represented by a string stretched between q and $\bar{q}$ endpoints of the cluster. Large clusters are split into smaller clusters which take for their motion the directions of the original cluster endpoints, i.e. along the string direction. Thus both models have string (or linear confinement) properties; as seen later, their predictions are very similar.

2 Data Sample and Event Selection

This analysis is based on the data collected with the DELPHI detector [6] at the CERN LEP collider from 1991 to 1994. The data were recorded at center-of-mass energies around 91.2 GeV. The present analysis relies on the information provided by the three cylindrical tracking detectors (Inner Detector, Time Projection Chamber (TPC), and Outer Detector) all operating in a 1.2 T magnetic field. The Inner Detector and TPC each cover the angular range $20° < \vartheta < 160°$, where ϑ is the polar angle with respect to the beam axis, and the Outer Detector covers the range $43° < \vartheta < 137°$.

The detection of multihadronic events uses charged particles and neutral clusters in the electromagnetic calorimeters [7]. The selection criteria for charged particles are that the momentum, p, should be above 0.4 GeV/c, the relative error on p less than 100%, the polar angle between 20° and 160°, and the track length above 30 cm. In addition, the impact parameter with respect to the beam in the plane perpendicular to the beam axis, and to the longitudinal coordinate at the origin, should be below 4 cm and 10 cm, respectively.

Hadronic events are selected by requiring at least six charged particles (with at least three in each hemisphere) and a total visible energy, E_{vis}, exceeding 20% of the c.m.s. energy. For good multiparticle acceptance the thrust axis is required to be at more than 50° to the beam. The thrust axis is defined as the direction that maximizes the sum of the absolute values of the longitudinal momenta of all the charged particles in the event. The number of events selected is $\sim$ 1.8 million.

3 Analysis

This analysis is a study of charged particle correlations in the rapidity variable with respect to the *thrust* direction. The thrust direction approximates the directions of the primary q and $\bar{q}$, especially for two-jet events. With all particles assumed to be pions, the rapidity, y, is defined as $\frac{1}{2}\ln((E+p_L)/(E-p_L))$, where p_L is the component of momentum parallel to the thrust axis, and E is the energy calculated using the pion mass.

To detect chain-like ordering of charge, first the *sign* of the charge of one of the primary quarks in the event is identified (or tagged). The charged particles in each event are ordered according to their rapidity values in the thrust direction, as shown in Fig. 1b. The 'tagged' particle (one for each hemisphere) is defined as the particle having the largest absolute value of rapidity in that hemisphere. Hemispheres are defined, one for positive y and one for negative y, with respect to the thrust direction.

To improve the efficiency for tagging the correct primary-quark charge, the rapidity gap adjacent to the tagged particle, Δy_{tag}, is required to be larger than a specified value, i.e. a 'tag condition'. A small rapidity difference between the leading and next-to leading particle would involve a larger probability for them to have 'crossed over', i.e. reversed rank. Zero, one or two tags are possible for a given event. Each hemisphere is considered independently. Later in this section, the more general case of tagging with more than one leading particle is considered.

The integer *rapidity-rank* (n_r) is defined as the position that a particle has in the rapidity chain when charged particles in the event are ordered according to their y values along the thrust axis. The counting for n_r begins at the end of the chain in each hemisphere (see Fig. 1b).

3.1 Compensating Charge $\Delta\rho(n_r)$

For the sample of N_{tag} tagged hemispheres, the average compensating charge at rapidity rank n_r is:

$$\Delta\rho(n_r) = \rho_o(n_r) - \rho_s(n_r), \tag{1}$$

where $\rho_o(n_r) = N_o(n_r)/N_{tag}$ and $N_o(n_r)$ is the number of particles at rank n_r with charge opposite to the tagged particle; $\rho_s(n_r)$ is defined similarly but for particles with the same charge. Charge conservation requires that the total charge of all the other particles in the event be minus the charge of the tagged particle. Of course, the reconstructed event will not always conserve charge because of possible missing tracks and secondary interactions.

Distributions in the variable $\Delta\rho(n_r)$ should reveal the nature and location in n_r of the charge compensation of the tagged particle. The distribution of $\Delta\rho(n_r)$ for three values of the Δy_{tag} requirement, (a) $\Delta y_{tag} > 0.5$, (b) $\Delta y_{tag} > 1.0$, and (c) $\Delta y_{tag} > 2.0$, is shown in Fig. 2. It is seen that for n_r near that of the tagged particle there is a large contribution of compensating charge, i.e. a short-range correlation (SRC); and at n_r furthest from the tagged particle in the opposite hemisphere there is evidence of a narrow-width correlation, called a long-range correlation (LRC) because of its distance from the tagged particle. The LRC is stronger (i.e. more fractional compensating charge) for the largest Δy_{tag} requirement, indicating that the primary parton charge is more efficiently tagged. The predictions for tagging efficiency (particle with largest rapidity in a hemisphere has the same sign of charge as the primary quark) from JETSET 7.3 for all Δy_{tag} and for $\Delta y_{tag} > 1.0$ are 56% and 64%, respectively. Also shown in Fig. 2 is a prediction of a random charge model, produced by randomizing the charges of particles in the data. The charges are randomized such that the net charge from reconstructed charged particles in each event is reproduced. This random charge model, although retaining the effects of charge conservation convoluted with the multiplicity distribution (because individual multiplicities have different ranges in n_r), does not reproduce the data.

The SRC is qualitatively consistent with local charge conservation, as expected from a string model and/or from resonance decays. The LRC provides evidence for the presence of charged primary partons, since tagging a given charge at one end of the rapidity chain yields a positive correlation for the opposite charge at the other end of the chain. Requiring larger values of Δy_{tag} greatly increases the observed strength of the LRC, and decreases the observed width of the SRC (from three to two rapidity-rank units). Since the average Δy, λ, is $\sim 1/2$ unit for rapidity gaps near the ends of the event, the width (half maximum) of each peak is estimated, from Fig. 2c, to be approximately one unit in y (two rapidity-rank units wide).

To increase the sensitivity for observing particles in their original rank order, the rapidity gaps Δy_i between the particle with rapidity-rank n_r and those at $n_r - 1$ and $n_r + 1$ are both required to exceed a given value. The rapidity gaps are defined as positive quantities. Generally, the requirement $\Delta y_i > 0.5$ is imposed but, to give 'equal' treatment to the particle with largest rapidity at the end of the chain ($n_r = 1$) and with only one adjacent gap, the requirement is doubled for this particle (i.e. to $\Delta y_i > 1.0$); this is somewhat arbitrary, but in accord with the assumption of an exponential rapidity-gap distribution, as seen in other data [9]. This adjacent-rapidity-gap condition is applied independently to each particle to include it in a distribution. It is not applied to the 'tagged' particle, which has separate requirements.

Distributions of $\Delta\rho(n_r)$ obtained after applying this condition are shown in Fig. 3 for (a) all Δy_{tag}, (b) $\Delta y_{tag} > 0.5$, and (c) $\Delta y_{tag} > 1.0$. These distributions are similar in shape to those of Fig. 2. However, a 'see-saw' effect can now be observed in the data furthest from the tagged particle in the opposite hemisphere. With the adjacent rapidity gap requirement and the Δy_{tag} cut, only a small number of charged particles are retained (e.g. 3% for Fig. 3b); however, capability to see charge structures in the data is attained. In general, the fraction of particles remaining after cuts on Δy_{tag} and Δy_i can roughly be estimated from a product of exponentials representing the rapidity-gap distributions, i.e. $\exp(-\Delta y_{tag}^{cut}/\lambda) \cdot [\exp(-\Delta y_i^{cut}/\lambda)]^2$, with $\lambda = \frac{1}{2}$. This formula assumes gap independence and somewhat overestimates the fraction in the data.

3.2 Compensating Charge Ratio $\mathcal{R}(n_r)$

In the following, the charge-compensation behavior is studied exclusively in the hemisphere opposite to that of the tagged particle. Detailed structures are difficult to observe in the tagged hemisphere because of the large amount of compensating charge resulting from local charge conservation to the tagged particle. It should be noted that this effect does *not* depend on having a correct tag of the primary quark charge. A large tagging efficiency for the incorrect charge results in a large background for the tagged hemisphere; thus, any detailed structure is effectively washed out. However, a very small 'alternation' in the tagged hemisphere may be seen in Fig. 3c, as evidenced by the fact that the $n_r = 4, 6$ points are significantly above a steeply falling smooth curve drawn through the $n_r = 3, 5, 7$ points. The opposite hemisphere, which is far from the effect of local charge conservation to the tagged particle, offers an unbiased situation for studying structure such as charge ordering.

To emphasize the relative difference between the opposite and same charges, the following ratio is introduced:

$$\mathcal{R}(n_r) = \Big(\rho_o(n_r) - \rho_s(n_r)\Big)\Big/\rho_o(n_r). \tag{2}$$

This ratio is shown in Fig. 4 for (a) all Δy_{tag}, (b) $\Delta y_{tag} > 0.5$, and (c) $\Delta y_{tag} > 1.0$. The adjacent rapidity gap condition described above is again applied. A strong oscillating pattern is seen which extends from the first particle in rapidity-rank to the sixth ($n_r = 1, \ldots, 6$). (Statistical uncertainties are too large beyond $n_r = 6$ to see any effect.) This type of behavior is the signature that would be expected for *chain-like charge-ordered* particle production in hadron jets. With larger Δy_{tag}, the data show an increased oscillation amplitude resulting from the better tagging efficiency.

The tagging method described above can be generalized to include more than one leading particle. If charge-ordering is valid, any odd number of leading charged particles can be used to identify the sign of a primary-quark charge. A group tag is considered when either three or five leading charged particles (i.e. those with the largest values of $|\, y \,|$ in a hemisphere) have net charge 1 (or -1) and rapidity-gap between the third (or fifth) particle and the following particle in the chain larger than a minimum value.

Fig. 5 shows the result for three (and five) leading particles, respectively, with the condition $\Delta y_{tag} > 0.5$. The alternating charge structure observed is similar to that seen for the case of a single leading particle. This gives further confirmation that charge-ordering exists locally over the entire rapidity chain.

Combining these tags, the event (each hemisphere) is tagged if the rapidity-gap is larger than a given value following the leading, or third, or fifth particle; only one entry per hemisphere is plotted. This gives the greatest number of tagged events. The ratio $\mathcal{R}(n_r)$ for the combined tag, with the same three Δy_{tag} conditions as in Fig. 4, is shown in Fig. 6. With the greater statistics, the alternating charge structure has increased significance.

Fig. 6 also compares the predictions of the Monte-Carlo models JETSET 7.3 and HERWIG 5.5 with the data. The generation parameters for JETSET 7.3 are given in table 10 of reference [8]. The HERWIG 5.5 event generation is done with default parameters, and the particle decays are treated by JETSET. Standard DELPHI detector simulation along with charged particle reconstruction and hadronic event selection are applied to the events from JETSET 7.3. The events from the HERWIG generation are not processed through the full detector simulation; instead a three-dimensional acceptance-probability function in momentum, azimuth and polar angles for charged particles, based on the ratio of accepted to generated particles in the JETSET simulation, is applied to each charged particle.[†] As seen in Fig. 6, both HERWIG and JETSET are in good agreement with the data.

[†]It has been checked that applying this rejection algorithm to an independent set of JETSET generated events reproduces the results from JETSET events processed with full detector simulation.

4 Conclusions

Evidence for chain-like charge-ordered particle production is observed in hadronic events from Z^0 decays. This confirms a fundamental and long-standing prediction of string-like fragmentation models. The weak coupling between the rank of a particle in the string and its position in the rapidity chain allow this effect to be studied. The JETSET and HERWIG models both agree with the data.

Acknowledgments

We are greatly indebted to our technical collaborators and to the funding agencies for their support in building and operating the DELPHI detector, and to the members of the CERN-SL Division for the excellent performance of the LEP collider.

References

[1] B. Andersson, G. Gustafson, G. Ingelman, T. Sjöstrand, Phys. Rep. **97** (1983) 31.
[2] R. P. Feynman and R. Field, Nucl. Phys. **B136** (1978) 1.
[3] TASSO Coll., R. Brandelik et al., Phys. Lett. **B100** (1981) 357;
AFS Coll., T. Akesson et al., Nucl. Phys. **B246** (1984) 408;
R. Moller, Acta Physica Polonica **B15** (1984) 989 (sect. 4.4).
[4] T. Sjöstrand and M. Bengtsson, Comp. Phys. Comm. **43** (1987) 367;
T. Sjöstrand, CERN-TH.6488/92, May 1992, Revised Sept. 1992.
[5] G. Marchesini and B. R. Webber, Nucl. Phys. **B238** (1984) 1;
B. R. Webber, Nucl. Phys. **B238** (1984) 492;
G. Abbiendi et al., Comp. Phys. Comm. **67** (1992) 465;
M. H. Seymour, in *Proceedings of the Workshop on Photon Radiation from Quarks*, Annecy France, 2-3 Dec. 1991, Ed. S. Cartwright, CERN 92-04, p. 113.
[6] DELPHI Coll., P. Aarnio et al., Nucl. Instr. and Meth. **A303** (1991) 233.
[7] DELPHI Coll., P. Aarnio et al., Phys. Lett. **B231** (1989) 539;
DELPHI Coll., P. Abreu et al., Phys. Lett. **B241** (1990) 435;
DELPHI Coll., P. Abreu et al., Z. Phys. **C53** (1992) 41;
DELPHI Coll., P. Abreu et al., Nucl. Phys. **B417** (1994) 3.
[8] DELPHI Coll., P. Abreu et al., Z. Phys. **C73** (1996) 11.
[9] M. Derrick et al., Z. Phys. **C35** (1987) 323.

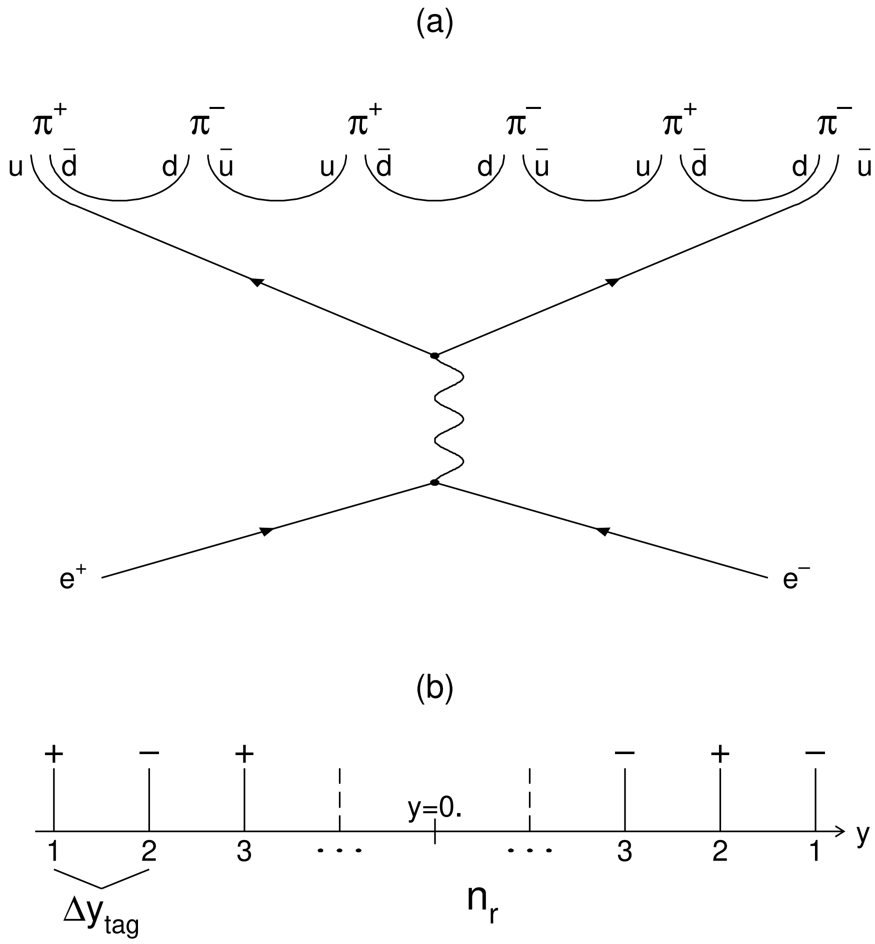

Figure 1: **(a)** Annihilation event with flavor-ordered chain production. The particles at the ends of the chain are 'rank 1', those adjacent are 'rank 2', etc. **(b)** Event with charged particles ordered according to their rapidity values in the thrust direction. The quantity n_r indicates the rapidity-rank, and Δy_{tag} is the rapidity gap adjacent to a 'tagged' particle ($n_r = 1$), shown here for one side.

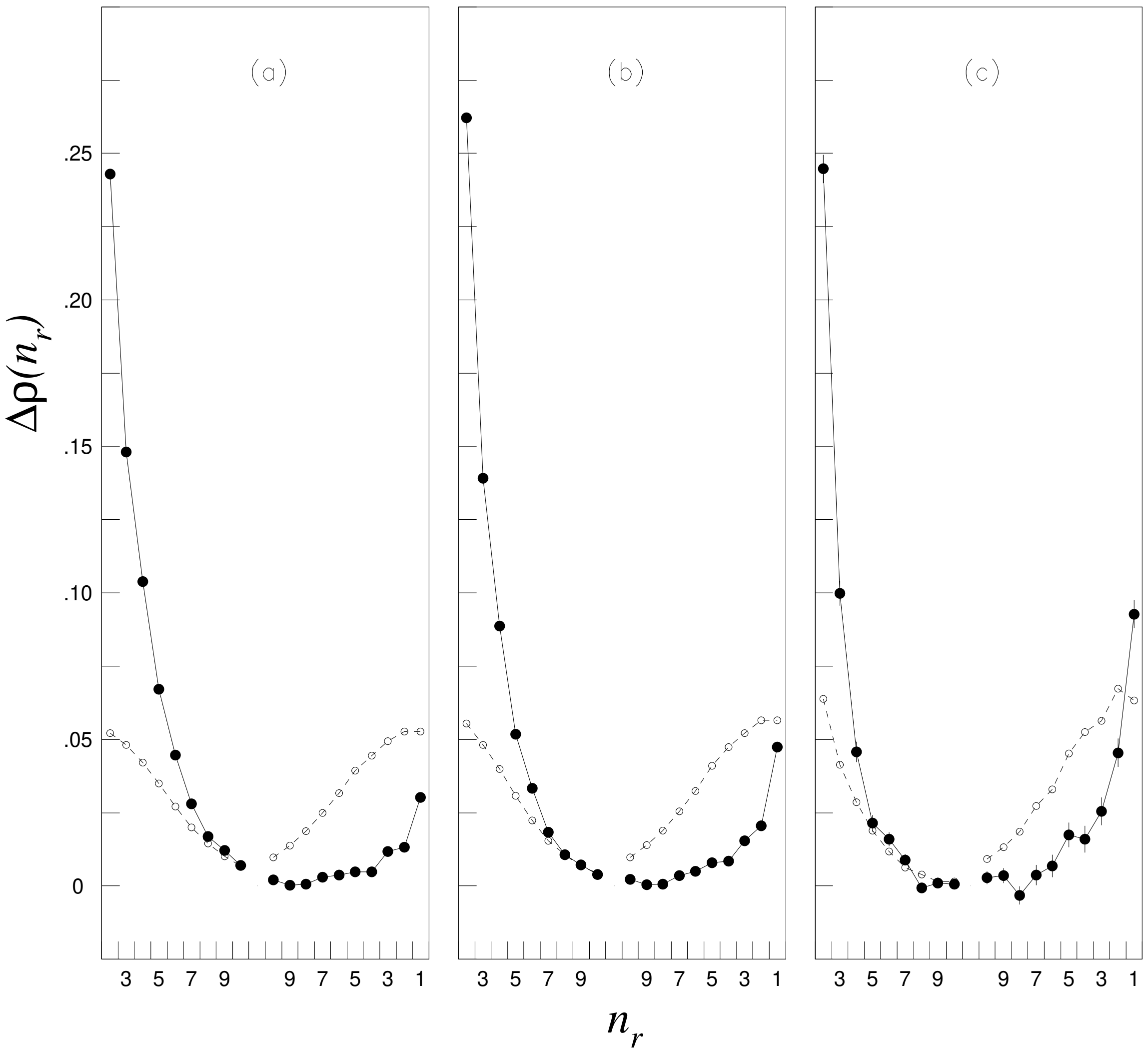

Figure 2: Compensating charge, $\Delta\rho(n_r)$, as a function of n_r ($n_r \leq 10$), for **(a)** $\Delta y_{tag} > 0.5$, **(b)** $\Delta y_{tag} > 1.0$, and **(c)** $\Delta y_{tag} > 2.0$. The tagged hemisphere is represented on the left side of each plot, starting with $n_r = 2$. The data point for the tagged particle ($n_r = 1$), which is equal to -1.0, is not shown. Data points ($\bullet\,'s$) are connected by solid lines. Predictions of a random charge model ($\circ\,'s$) are connected by dashed lines.

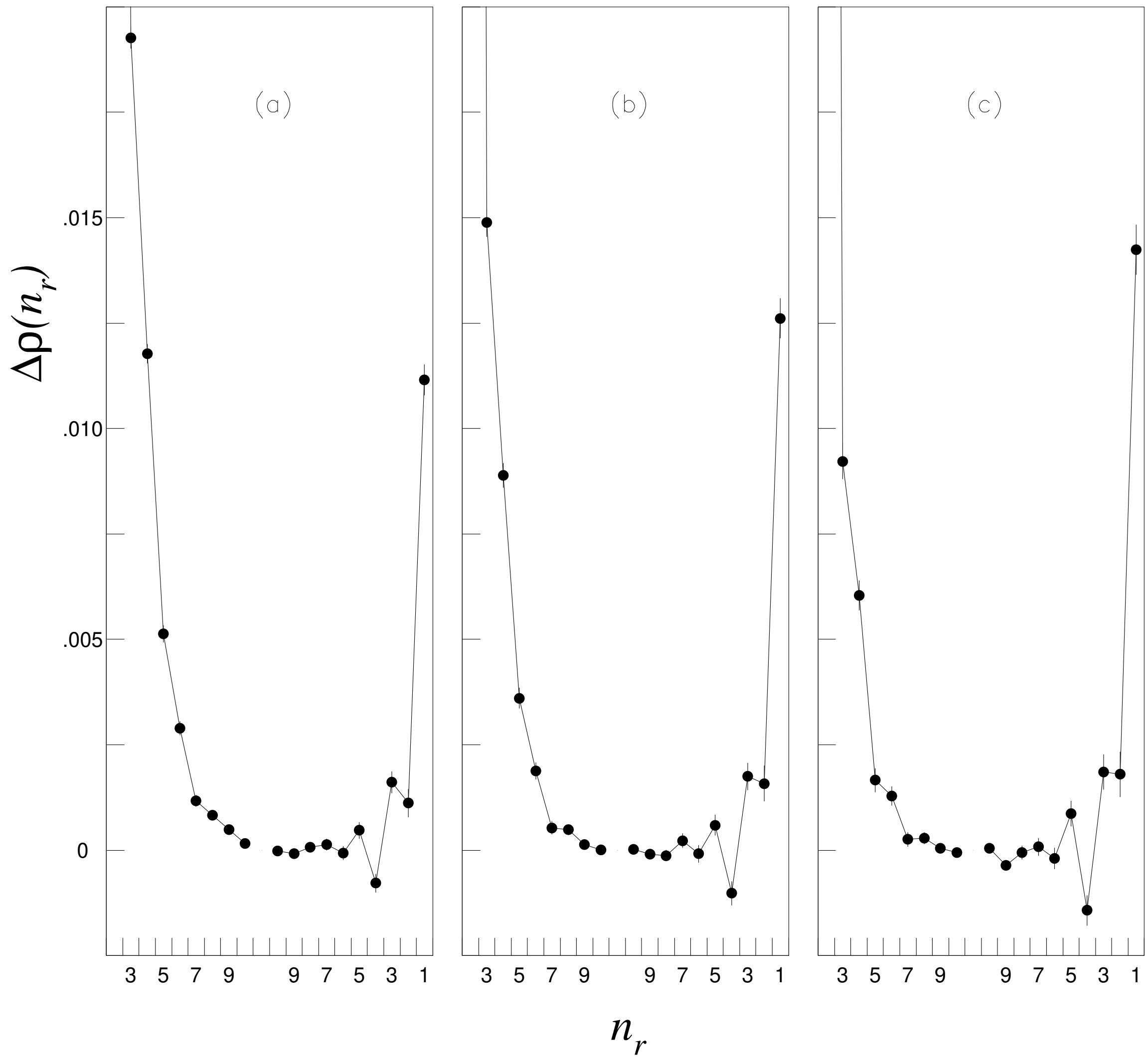

Figure 3: Compensating charge, $\Delta\rho(n_r)$, as a function of n_r ($n_r \leq 10$), for **(a)** all Δy_{tag}, **(b)** $\Delta y_{tag} > 0.5$, and **(c)** $\Delta y_{tag} > 1.0$, with the adjacent-rapidity-gap condition $\Delta y_i > 0.5$ (1.0) applied. The tagged hemisphere is again represented on the left side of each plot, but the data points $n_r = 2$ (values 0.071, 0.143, and 0.115 for (a), (b), and (c), respectively) are not shown in order to accommodate an expanded scale.

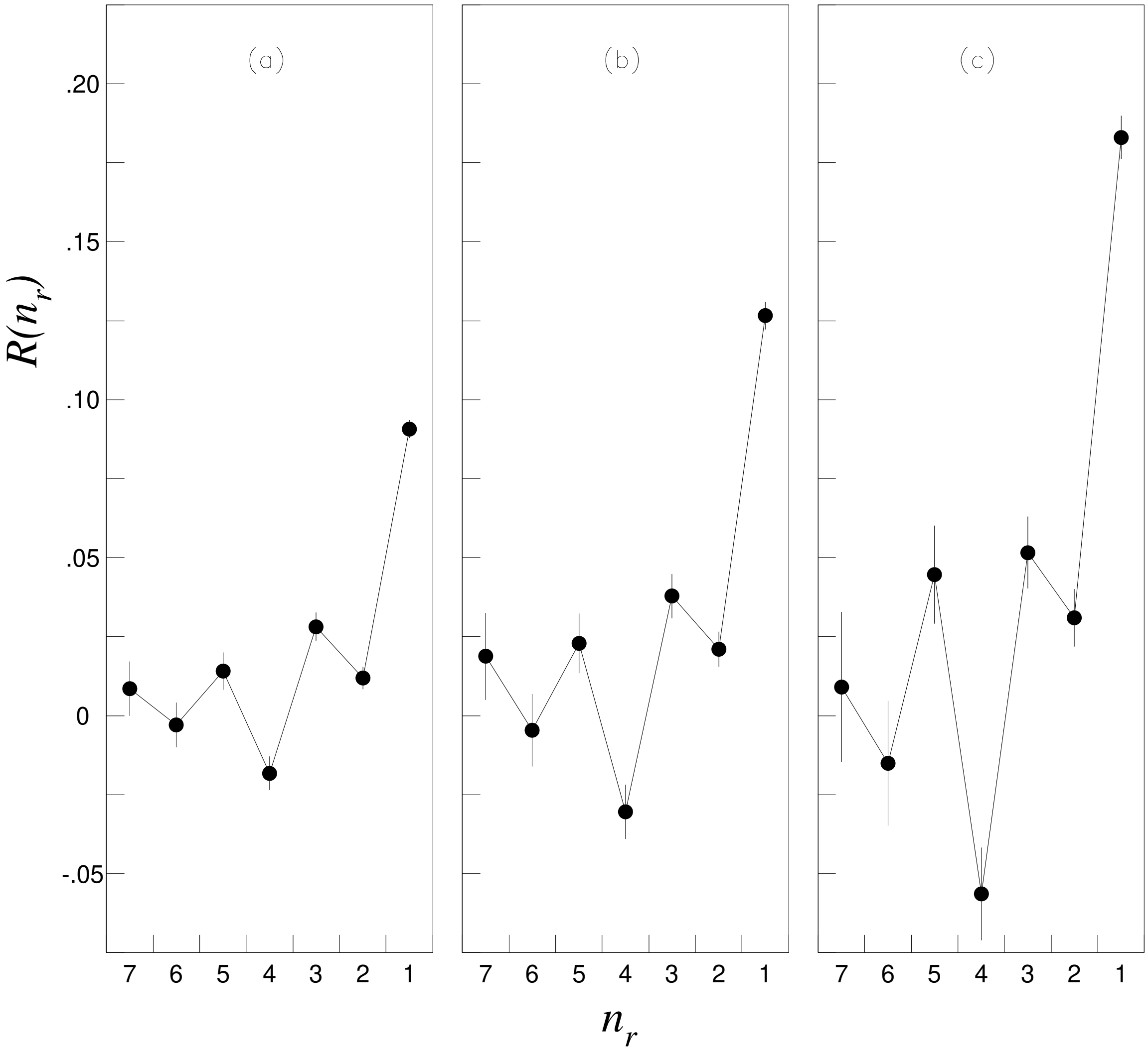

Figure 4: Compensating-charge ratio, $\mathcal{R}(n_r)$, as a function of n_r for **(a)** all Δy_{tag}, **(b)** $\Delta y_{tag} > 0.5$, and **(c)** $\Delta y_{tag} > 1.0$, for the hemisphere opposite to the tagged particle. The adjacent-rapidity-gap condition is applied. The points for $n_r > 7$ have large uncertainties and are not shown.

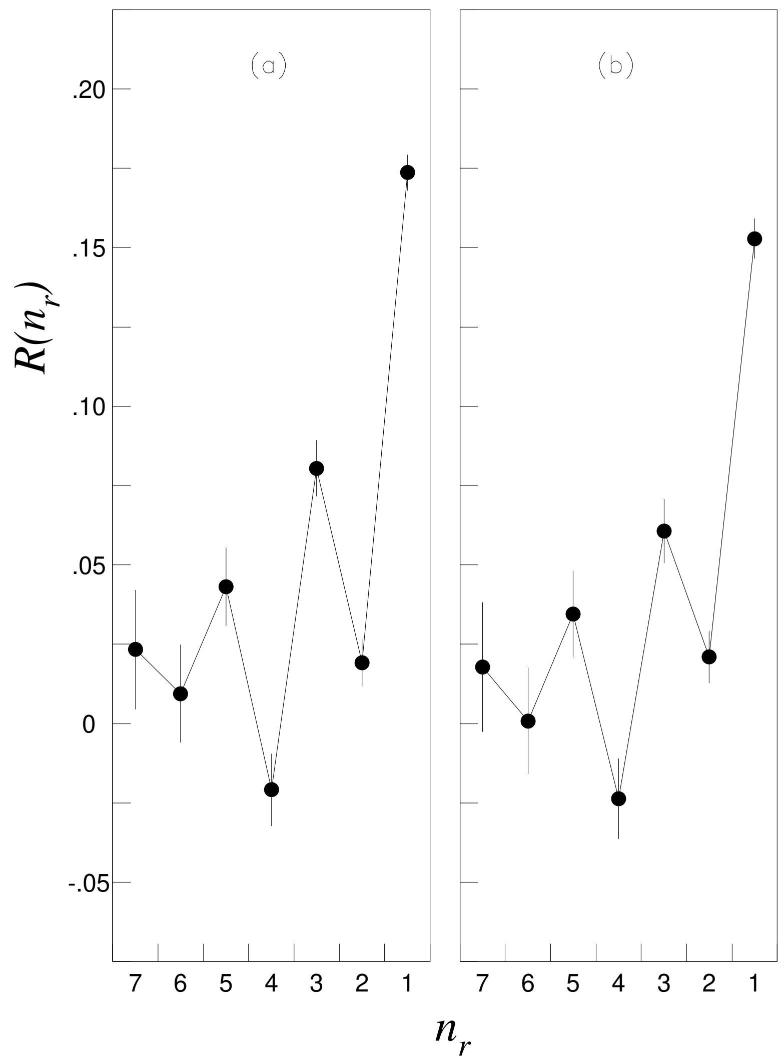

Figure 5: Compensating-charge ratio, $\mathcal{R}(n_r)$, as a function of n_r with $\Delta y_{tag} > 0.5$, for **(a)** the three-leading-particle tag, and **(b)** the five-leading-particle tag. The adjacent-rapidity-gap condition is applied.

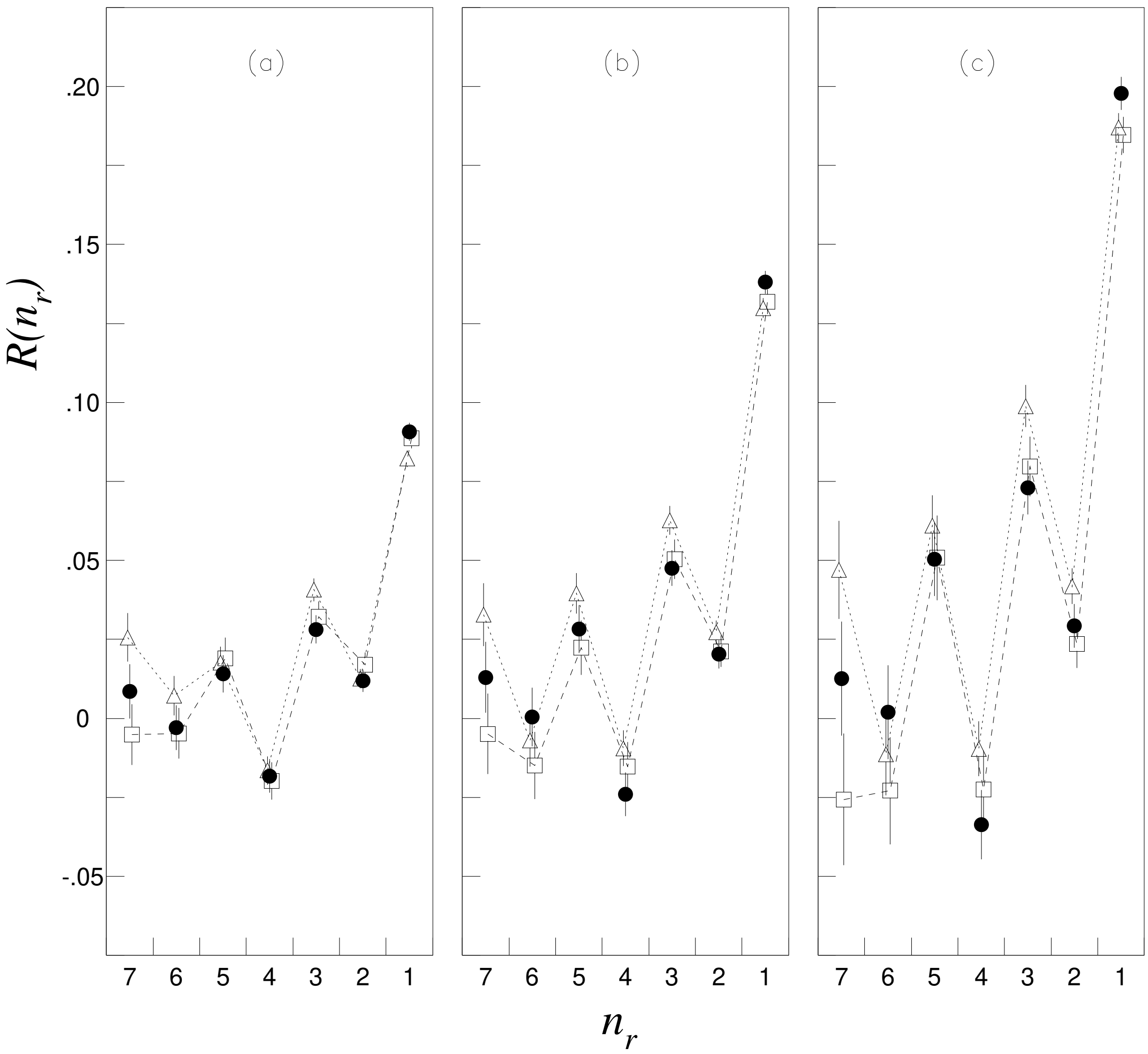

Figure 6: Compensating-charge ratio, $\mathcal{R}(n_r)$, as a function of n_r for **(a)** all Δy_{tag}, **(b)** $\Delta y_{tag} > 0.5$, and **(c)** $\Delta y_{tag} > 1.0$, for the combined case of tagging single, three, or five leading particles. The adjacent-rapidity-gap condition is applied. The data points ($\bullet$'s) are shown unconnected. The predictions of JETSET 7.3 ($\square$'s) and HERWIG 5.5 ($\triangle$'s) are connected by dashed and dotted lines, respectively.